*Advances in Animal Biosciences: Precision Agriculture (ECPA) 2017*, (2017), **8:2**, pp 837–841 © The Animal Consortium 2017
doi:10.1017/S2040470017001340

advances in animal biosciences

# Simulation and Experiment of a Designed Anti-Drift Spray Nozzle

W. Deng†, C. Zhao, L. Chen and R. Zhang

*National Engineering and Research Centre for Information Technology in Agriculture, Nongke Mansion, No.11 Shuguang Hua Yuan Middle Road, Haidian District, Beijing 100097,P.R.China*

*This paper reports an investigation of the relationship between spray characteristics and a nozzles' internal structure to reveal the working mechanism of anti-drift spray nozzles. Three important structural factors were taken into account, the diameter of the inner chamber, the angle of V-shaped slot and the relative kerf depth. Three-dimensional models of the fan nozzles were set up using Solidworks software and the corresponding real nozzles were produced using high-precision 3-D printer. The flow fields inside the nozzles were simulated using the software FLUENT. By comparing the flow fields inside and outside the nozzles under the conditions of the same inner structural parameter, the relationships between spraying flow characteristics and different structural parameters was made clear, and provides a reference for optimal design of anti-drift spray nozzles.*

**Keywords:** Inner structure, FLUENT, Spray angle, spray pressure

## Introduction

China is currently the world leader in pesticide utilization. According to national statistics, the annual area sprayed with pesticide has reached 167 million ha, of which about 13.3 million ha (or one-seventh) is polluted by pesticide. Related research shows that less than 0.03% of the pesticides applied can make a real impact on killing insects, while more than 20% to 30% of pesticide droplets sprayed from sprayers drift to non-target areas with airflow. The non-targeted drift of pesticide droplets is the key reason causing the serious loss of pesticides, environmental pollution, and low disease-controlling effect (Liu *et al*., 2005; Qi *et al*., 2002; Song *et al*., 2011; He 2004; Yuan *et al*., 2011; Yang *et al*., 2002; Wang *et al*., 2014; Dong *et al*., 2012).

The spray nozzle is one of the most important components for realizing effective and precise chemical application with sprayers because it plays an important role during the atomization of pesticide solutions (Fan *et al*., 2014; Xie *et al*., 2013). At present, research on nozzle technologies is still in continuous improvement and development and the understanding of certain nozzle constructions and their mechanism is still being explored. A previous study on spray nozzles used for plant protection, mainly depended on actual experiments to assess spray characteristics using some intuitive measurements methods that were associated with a high cost, long test cycle, heavy workload and complex test procedure (Hou and Hou 2002). In recent years, with the rapid development of computer technology and theory research on computational fluid dynamics (CFD), it has been a trend to simulate the atomization process and the spray characteristics of nozzles by means of computer numerical simulation. CFD method can overcome some shortcomings of traditional experimental methods and provide an intuitive understanding of the details of flow fields inside and outside nozzles via simulation, such as the change of pressure, velocity, and temperature, and the feature of velocity vectors in flow fields (Yang *et al*., 2008). The corresponding flow field can be rapidly observed when the external conditions are changed, so that interference from uncontrollable factors in field experiments to experimental results can be avoided; which cannot be achieved by the traditional experimental method (Fu *et al*., 2009; Sidamed and Brown 2001; Xu *et al*., 1998; Ning and Pang 2006; Qi *et al*., 2010). Therefore simulating the spray flow field is a great support to precision chemical application.

In this paper, an anti-drift fan spray nozzle was designed. The geometric model of the fan nozzle was established using the 3D design software 'Solidworks' and the nozzle was fabricated using high precision 3D printing technology. The influences of nozzle inner-structure factors on pressure and velocity flow-fields were studied through computer simulation technology and the effect of the inner-structure factors on spray angle, which is a key spray characteristics, were studied in experiments. According to the literature (Deng *et al*., 2006), spray pressure is the decisive factor in determining spray angle. The results of the simulation and experimental tests on the nozzle's flow field were compared to provide a theoretical basis for optimal design of anti-drift spray nozzles.

† E-mail: dengw@nercita.org.cn



https://doi.org/10.1017/S2040470017001340 Published online by Cambridge University Press

## Materials and methods

*The inner structure of fan nozzle*

The inner structure of the fan nozzle was designed and is shown in Figure 1. In the structure diagram, *h*, on behalf of the hole-edge distance, is the distance between the end of the spray orifice and the transverse plane of the spray nozzle. *e* is for the over-center distance. *H* represents the groove depth. α is for the opening angle of the V-shaped groove. *r* is for the curve radius of the nozzle end's shape. *d* is the diameter of nozzle chamber. *l* is the lumen length of the orifice end. $H_r$, for the relative cutting depth, is the parameter used for manufacturing nozzles and reflects the relative depth of the cutting on the ball surface of nozzle's head in the process of nozzle manufacturing. The equation of calculating $H_r$ is shown in Formula (1).

$$H_r = \frac{r-e}{r} = \frac{H-h}{r} = \frac{2(H-h)}{d} \quad (1)$$

According to a large number of experimental results, the diameter of nozzle chamber (*d*), the opening angle of V-slot (α), and the relative cutting depth ($H_r$) are the important structural parameters of nozzles that affect spray characteristics (Huang 2014; Liu 2007). Therefore, the focus here is on the influence of these three structural parameters on a nozzles' spray characteristics.

*Analogue simulation*

*Geometric model and mesh generation*. The geometry model of a nozzle was established in Solidworks, and used as an inpu into the FLUENT software. The model was meshed using a volume meshing method in which grid elements were Hex/Wedge (mainly hexahedral mesh at most positions, wedge-shaped grid at some local positions). The grid type was Cooper and the interval size was 0.1. The outlet end of spray orifice was also meshed with Tet/Hybrid grid elements, TGrid grid type, and local mesh refinement.

*The model of fluid computation*. A standard *k-ε* turbulence model (Sun *et al*., 2012) was adopted to establish mathematical equations in this study. In the FLUENT software, the finite volume method is adopted for dissociation of control equations and the SIMPLE algorithm is used for calculation.

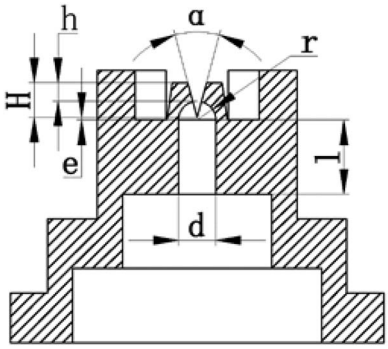



**Figure 1** Profile diagram of nozzle structure

Simulation parameters were defined as follows. The inlet pressure was 0.3 MPa and the outlet pressure was atmospheric pressure. The density and the viscosity of the single-phase liquid water which was used as flowing medium is 998.2 kg/m$^3$ and 0.001 Pa·s. The liquid-solid interface was set to be a non-slip boundary condition. The solver was selected as a pressure-based algorithm. The turbulence intensity and hydraulic diameter were used as boundary conditions to define the turbulence parameters, and the turbulence intensity and the hydraulic diameter were set to 5% of the diameter of the nozzle's orifice.

*Simulation*. Three factors, namely, lumen diameter, V-shaped groove angle, and relative cutting depth, were selected in the analogue simulation. Three tests were designed where one factor was changed while keeping the other two factors unchanged. The input parameters for the three tests are shown in Tables 1–3. Test 1 changed the lumen diameter while keeping the V-shaped groove angle and relative cutting depth unchanged. Test 2 changed the V-shaped groove angle while keeping the lumen diameter and relative cutting depth unchanged. Test 3 changed the relative cutting depth while keeping the lumen diameter and V-shaped groove angle unchanged. For each test, 6 kinds of nozzles with different inner structures were fabricated and the corresponding nozzle models were input into FLUENT and simulated to verify the influence of each factor on the flow field inside the nozzle.

In the simulation, images of pressure and velocity fields on the center plane inside the nozzle were obtained. Because the images of pressure and velocity fields cannot be effectively compared, the pressure and velocity data on the central axis of each nozzle model were respectively extracted from the FLUENT software, imported into MATLAB software, and drawn as pressure and velocity curves using the graphic function in MATLAB to compare the pressure and velocity inside each nozzle and to lead to valid conclusions.

*Spraying test*

*Test equipment and materials*. The nozzles used in the study were fabricated using a 3D printing technique using the structure in Figure 1 and according to the dimensions shown in Tables 1–3. The printing material was a photosensitive resin with a printing accuracy of 25 μm. The test device for measuring nozzle integrative performances was composed of a water pump, control switch, regulating valve, power supply, liquid tank, pressure gauge, nozzles, water pipes, and other devices. The total capacity of the spray tank was 50 L. The regulating range of the nozzle's height was 1000 mm. The maximum flow rate and pressure were respectively 5 L/min and 2 MPa. The temperature was 10 ~ 35°C and the relative humidity > 50%.

*Test method*. Spray angle is one of the important parameters to characterize the spray performance of a nozzle. The spray angles of each nozzle printed using 3-D printing technology were measured in turn on the testbed and calculated using



https://doi.org/10.1017/S2040470017001340 Published online by Cambridge University Press

the image-identified method (Deng *et al*., 2006). Three tests were carried out as shown in Table 1 (the only change of lumen diameter), Table 2 (the only change of V-shaped groove angle), and Table 3 (the only change of relative cutting depth). In all tests, the spray pressure was set to be 0.3 MPa, the height of the nozzle above the testbed was 50 cm. For each test, the system was 'shot' three times at intervals of 5 minutes and the average value of the three measured spray angles was regarded as the final measurement of spray angle for certain test conditions.

## Results and discussion

*Simulation*

*Influence of cavity diameter on inner flow field*. The 6 nozzle models were respectively established according to the structural parameters shown in Table 1 (Simulation 1) and were imported into FLUENT software after being divided into grids using Gambit software. The result shows that the changing trends of pressure and velocity curves along the axis line of the six nozzles are basically the similar. The pressure decreases and the velocity increases with the increasing distance from the center to the bottom along the axis of the nozzle. It shows that six pressure curves basically overlap together while the velocity curves increase slightly with an increase in the lumen diameter, which indicates that the nozzle's cavity diameter has a certain influence on the velocity of the flow field inside the nozzle.

*Influence of V-shaped groove angle on inner flow field*. For the second simulation (Table 2 parameters), with a changing of V-shaped groove angle inside the nozzle, the pressure and velocity curves along the center axes of the six fabricated was basically consistent. With an increase of distance from the center to the bottom along the axis inside the nozzle, the pressure decreased and the velocity increased. Meanwhile, the pressure gradually decreased and the velocity slightly increased with the increase of the V-shaped groove angle, with little change in the range of the inner flow field of the six nozzles.

*Influence of relative cutting depth on inner flow field*. When altering the relative cutting depth (Table 3), the trends of pressure and velocity curves along the center axis of the six nozzles were similar. When the distance from the center to the bottom of the nozzle is less than 6 mm, the pressure and velocity is essentially unchanged; while when the distance is more than 6 mm, the liquid pressure drops and the velocity rises rapidly. Furthermore, the greater the relative cutting depth, the faster the liquid pressure dropped and the liquid velocity increased. When the distance is more than 9 mm, the influence of the relative cutting depth on the inner pressure and velocity of nozzles became smaller. With further increase of relative cutting depth, the inner liquid pressures of the six nozzles approached the same value and decreased sharply, meanwhile the inner liquid velocity of the six nozzles approached the same value.

*Spray test*

*Influence of cavity diameter on spray angle*. Keeping the V-shaped groove angle and the relative cutting depth unchanged, respectively at 30° and 0.8, the six nozzles with different cavity diameters fabricated in Test 1 were used in the spray test and the test results are shown in Table 4. It can be seen that the spray angle tended to increase with an increase of cavity diameter. The test result is in accordance with the simulation above. It indicated that increasing of nozzle's cavity diameter increased the fluid velocity slightly and made the spray angle increase. The results showed that with an increase in cavity diameter, the resistance inside the nozzle decreased while the liquid velocity increased. Therefore, the radial velocity component accordingly increased resulting in an increased spray angle.

*Influence of V-shaped groove angle on spray angle*. Keeping the cavity diameter and the relative cutting depth unchanged,

**Table 1** *The change of cavity diameter*

| Sequence number of nozzles | Cavity diameter (mm) | V-shaped groove angle (°) | Relative cutting depth (mm) |
|---|---|---|---|
| 1 | 1.5 | 30° | 0.8 |
| 2 | 1.7 | 30° | 0.8 |
| 3 | 2.0 | 30° | 0.8 |
| 4 | 2.3 | 30° | 0.8 |
| 5 | 2.5 | 30° | 0.8 |
| 6 | 2.8 | 30° | 0.8 |

**Table 2** *The change of V-shaped groove angle*

| Sequence number of nozzles | V-shaped groove angle (°) | Cavity diameter (mm) | Relative cutting depth (mm) |
|---|---|---|---|
| 7 | 30° | 2.0 | 1 |
| 8 | 35° | 2.0 | 1 |
| 9 | 45° | 2.0 | 1 |
| 10 | 60° | 2.0 | 1 |
| 11 | 70° | 2.0 | 1 |
| 12 | 80° | 2.0 | 1 |

**Table 3** *The change of relative cutting depth*

| Sequence number of nozzles | Relative cutting depth (mm) | Cavity diameter (mm) | V-shaped groove angle (°) |
|---|---|---|---|
| 13 | 0.5 | 2.0 | 30° |
| 14 | 0.8 | 2.0 | 30° |
| 15 | 1.0 | 2.0 | 30° |
| 16 | 1.2 | 2.0 | 30° |
| 17 | 1.4 | 2.0 | 30° |
| 18 | 1.5 | 2.0 | 30° |



https://doi.org/10.1017/S2040470017001340 Published online by Cambridge University Press

**Table 4** *The spray angle of each nozzle with a changing cavity diameter*

| Sequence number of nozzles | Cavity diameter (mm) | V-shaped groove angle = 30° Relative cutting depth = 0.8 mm Measurements of spray angle 1 | 2 | 3 | Average spray angle (°) |
|---|---|---|---|---|---|
| 1 | 1.5 | 83.45° | 85.30° | 84.12° | 84.29° |
| 2 | 1.7 | 89.16° | 86.27° | 88.84° | 88.09° |
| 3 | 2.0 | 95.72° | 93.85° | 96.14° | 95.24° |
| 4 | 2.3 | 96.78° | 97.58° | 98.80° | 97.72° |
| 5 | 2.5 | 102.31° | 105.47° | 104.13° | 103.97° |
| 6 | 2.8 | 89.71° | 90.42° | 91.36° | 90.50° |

**Table 5** *The spray angle of each nozzle with the change of V-shaped groove angle*

| Sequence number of nozzles | V-shaped groove angle/ ° | Cavity diameter = 2 mm Relative cutting depth = 1 Measurements of spray angle 1 | 2 | 3 | Average spray angle/° |
|---|---|---|---|---|---|
| 7 | 30° | 106.43° | 110.31° | 109.08° | 108.61° |
| 8 | 35° | 95.41° | 98.62° | 97.16° | 97.06° |
| 9 | 45° | 85.12° | 86.70° | 84.53° | 85.45° |
| 10 | 60° | 73.45° | 79.81° | 76.78° | 76.68° |
| 11 | 70° | 59.24° | 60.34° | 58.67° | 59.42° |
| 12 | 80° | 56.13° | 50.42° | 55.34° | 53.96° |

**Table 6** *The changing curve of spray angle to the nozzle's relative cutting depth*

| Sequence number of nozzles | Relative cutting depth | Cavity diameter = 2 mm V-shaped groove angle = 30° Measurements of spray angle 1 | 2 | 3 | Average spray angle/° |
|---|---|---|---|---|---|
| 13 | 0.5 | 80.16° | 82.38° | 83.56° | 82.03° |
| 14 | 0.8 | 95.72° | 93.85° | 96.14° | 95.24° |
| 15 | 1.0 | 106.43° | 110.31° | 109.08° | 108.61° |
| 16 | 1.2 | 108.51° | 111.20° | 109.44° | 109.72° |
| 17 | 1.4 | 115.37° | 114.16° | 113.79° | 114.44° |
| 18 | 1.5 | 110.27° | 109.85° | 110.48° | 110.20° |

respectively to be 2 mm and 1, the test results from the six nozzles with different V-shaped groove angles fabricated (Table 2) are shown in Table 5. It can be seen that the spray angle gradually decreased with increased V-shaped groove angle. This test result is in accordance with the simulation result above. An increase of the nozzle's V-shaped groove angle decreased the fluid pressure and decreased the spray angle.

The results also showed that the constraint force on the fluid received from the V-shaped groove wall at the nozzle exit decreased with an increased V-shaped groove angle, and the fluid pressure accordingly decreased. This process is probably accompanied by an enhancement of liquid surface tension so that the liquid flow became more concentrated and the spray angle reduced.

*Influence of relative cutting depth on spray angle*. The test results when keeping the cavity diameter and the V-shaped groove angle unchanged, respectively to be 2 mm and 30°, are shown in Table 6. It can be seen from Table 6 that the spray angle gradually increased with increased relative cutting depth. However, the spray angle has a decreasing tendency when the relative cutting depth increased to a certain extent. This test result is similar to the simulation



https://doi.org/10.1017/S2040470017001340 Published online by Cambridge University Press

results above. It demonstrated that an increased relative cutting depth decreased the fluid pressure while fluid velocity increased. The influence of pressure and velocity on the spray angle will be mutually offset. It is probably because of the change of relative cutting depth that led to a change of liquid surface tension, resulting in a changed spray angle.

## Conclusions

The 3-D models of the fan nozzles were developed using Solidworks software and the influence of nozzle's design parameters, mainly as cavity diameter, V-shaped groove angle, and relative cutting depth, on the flow field inside the nozzle were simulated using the software FLUENT. The simulation results showed that the V-shaped groove angle and the relative cutting depth had greater influence on the fluid pressure and velocity inside the nozzle than the cavity diameter of the nozzle. With an increased cavity diameter, fluid pressure inside the nozzle was basically unchanged while the velocity increased slightly. With an increased V-shaped groove angle, the inner fluid pressure gradually decreased and the inner fluid velocity gradually increased. With increased relative cutting depth, the inner fluid pressure sharply decreased while the fluid velocity increased.

The spray nozzles with different design parameters were fabricated using high-precision 3-D printing technology and the influences of nozzle's design parameters on spray angle were tested on a spray test-bed. The test results revealed that the spray angle had an increasing tendency with increased cavity diameter, gradually decreased with an increased V-shaped groove angle, and gradually increased with an increased relative cutting depth. In particular, there was a reduced trend for the spray angle when the relative cutting depth increased to a certain extent.

## References

Deng W, Ding WM, Liu P and Zhang H 2006. A method of processing the atomization image and detecting the spray angle. Journal of Northwest Sci-Tech University of Agriculture and Forest (natural science edition) 34 (7), 155–159.

Dong X, Yang XJ and Yan HR 2012. Three-dimensional simulation on drift-reduction of air-assist spraying. Journal of Agricultural Mechanization Research 9, 44–48. (in Chinese with English abstract).

Fan R, Shi SB and Yang FZ 2014. Research status and development trends on nozzles used in plant protection machinery. Journal of Agricultural Mechanization Research 6, 6–9. (in Chinese with English abstract).

Fu ZT, Wang J and Qi LJ 2009. CFD simulation and experimental verification of air-velocity distribution of air-assisted orchard sprayer. Transactions of the Chinese Society of Agricultural Engineering 25 (01), 69–74. (in Chinese with English abstract).

He XK 2004. Improving severe draggling actuality of plant protection machinery and its application techniques. Transactions of the Chinese Society of Agricultural Engineering 20 (1), 13–15. (in Chinese with English abstract).

Hou LY and Hou XC 2002. Technical manual of nozzle Beijing: China petrochemical press, pp 309–317.

Huang FG 2014. Parametric design of plant protection nozzle. Yangling: Northwest A&F University (in Chinese with English abstract).

Liu XJ, Zhou HP and Zheng JQ 2005. Research advances of the technologies for spray drift control of pesticide application. Transactions of the Chinese Society of Agricultural Engineering 21 (01), 186–190. (in Chinese with English abstract).

Liu PZ 2007. Design of distribution bench for precision measuring spray nozzle integrative performance and on fan spray nozzle. Nanjing: Nanjing Agricultural University, (in Chinese with English abstract).

Ning DL and Pang FG 2006. Numerical simulation of air-blast nozzle use of fluent: The third conference on computational fluid mechanics, Harbin. pp. 653–659.

Qi LJ, Fu ZT and Shi Y 2002. Technology of pesticide application and food security. Transactions of the Chinese Society of Agricultural Engineering 18 (06), 203–206. (in Chinese with English abstract).

Qi LJ, Zhao YQ and Wang J 2010. CFD simulation and experimental verification of droplet dispersion of air-assisted orchard sprayer. Transactions of the Chinese Society of Agricultural Machinery 41 (02), 62–67. (in Chinese with English abstract).

Sidamed MM and Brown RB 2001. Simulation of spray dispersal and deposition from a forestry airblast sprayer Part II: Droplet trajectory model. Transactions of the American Society of Agricultural Engineers 44 (1), 5–7.

Song JL, Liu YJ and Zhang J 2011. Drift mechanism of flat fan nozzle. Transactions of the Chinese Society of Agricultural Machinery 42 (06), 63–69. (in Chinese with English abstract).

Sun GX, Wang XC and Ding WM 2012. Simulation analysis on characteristics of droplet deposition base on CFD discrete phase model. Transactions of the Chinese Society of Agricultural Engineering 28 (06), 13–19. (in Chinese with English abstract).

Wang XN, He XK and Herbst A 2014. Development and performance test of spray drift test system for sprayer with bar. Transactions of the Chinese Society of Agricultural Engineering 30 (18), 55–62. (in Chinese with English abstract).

Xie C, He XK and Song JL. 2013. Comparative research of two kinds of flat fan nozzle atomization process. Transactions of the Chinese Society of Agricultural Engineering 29 (05), 25–30. (in Chinese with English abstract).

Xu ZG, Walklate PJ and Rigby SG 1998. Stochastic modeling of turbulent spray dispersion in the near-field of orchard sprayers. Journal of Wind Engineering and Industrial Aerodynamics 74-76, 295–304.

Yang GL, Zhou WH and Liu F 2008. Simulation of flow field of high-pressure water-jet from nozzle with FLUENT. Journal of Lanzhou University of Technology 34 (02), 49–52. (in Chinese with English abstract).

Yang XJ, Yan HR and Xu SZ 2002. Current situation and development trend of equipment for crop protection. Transactions of the Chinese Society of Agricultural Machinery 33 (6), 129–131. (in Chinese with English abstract).

Yuan HZ, Yang DB and Yan XJ 2011. Pesticide efficiency and the way to optimize the spray application. Plant Protection 37 (05), 14–20. (in Chinese with English abstract).



https://doi.org/10.1017/S2040470017001340 Published online by Cambridge University Press